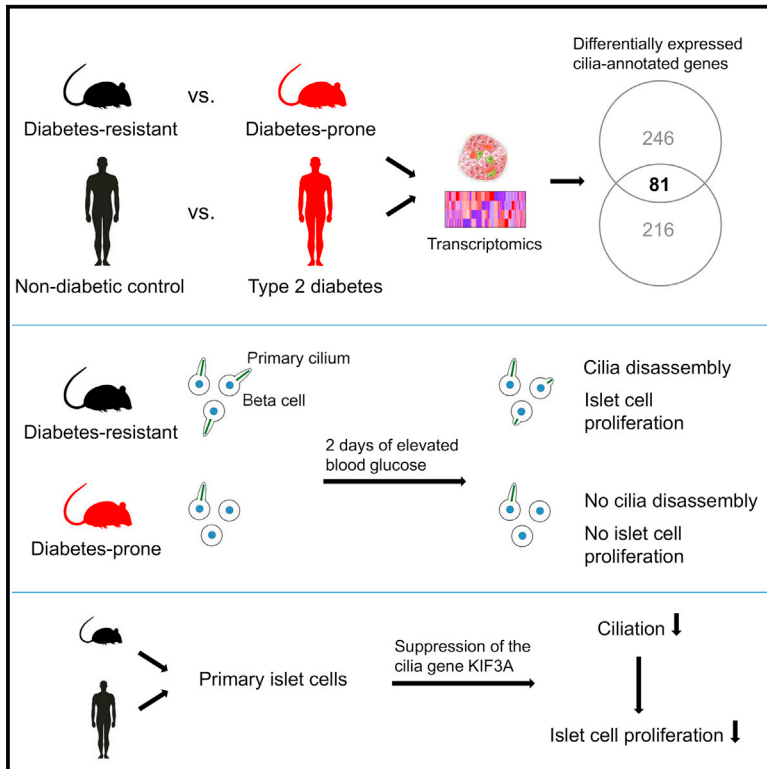


Decreased Expression of Cilia Genes in Pancreatic Islets as a Risk Factor for Type 2 Diabetes in Mice and Humans

Graphical Abstract



Authors

Oliver Kluth, Mandy Stadion, Pascal Gottmann, ..., Charlotte Ling, Jantje Gerdes, Annette Schürmann

Correspondence

schuermann@dife.de

In Brief

Kluth et al. identify a significant enrichment of cilia-annotated genes that are differentially expressed in pancreatic islets of obese mice. Many of the genes were also linked to human T2D, suggesting that dysregulation of cilia-associated genes may participate in T2D risk.

Highlights

- Differential expression of cilia-annotated genes in islets of diabetic mice and humans
- Islets of control mice have more cilia, which disassemble under high glucose levels
- Pathway enrichment analysis links affected cilia genes to cell division
- Inhibition of KIF3A lowers islet cell replication in mice and humans



Decreased Expression of Cilia Genes in Pancreatic Islets as a Risk Factor for Type 2 Diabetes in Mice and Humans

Oliver Kluth,^{1,2,7} Mandy Stadion,^{1,2,7} Pascal Gottmann,^{1,2} Heja Aga,^{1,2} Markus Jähnert,^{1,2} Stephan Scherneck,^{1,3} Heike Vogel,^{1,2} Ulrika Krus,⁴ Anett Seelig,^{2,5} Charlotte Ling,⁴ Jantje Gerdes,^{2,5} and Annette Schürmann^{1,2,6,8,*}

¹Department of Experimental Diabetology, German Institute of Human Nutrition Potsdam-Rehbruecke (DIfE), Nuthetal, Germany

²German Center for Diabetes Research (DZD), München-Neuherberg, Germany

³Institute of Pharmacology, Toxicology and Clinical Pharmacy, University of Braunschweig, Braunschweig, Germany

⁴Department of Clinical Sciences, Lund University, Malmö, Sweden

⁵Institute for Diabetes and Regeneration Research, Helmholtz Center Munich, Munich, Germany

⁶University of Potsdam, Institute of Nutritional Sciences, Nuthetal, Germany

⁷These authors contributed equally

⁸Lead Contact

*Correspondence: schuermann@dife.de

<https://doi.org/10.1016/j.celrep.2019.02.056>

SUMMARY

An insufficient adaptive beta-cell compensation is a hallmark of type 2 diabetes (T2D). Primary cilia function as versatile sensory antennae regulating various cellular processes, but their role on compensatory beta-cell replication has not been examined. Here, we identify a significant enrichment of downregulated, cilia-annotated genes in pancreatic islets of diabetes-prone NZO mice as compared with diabetes-resistant B6-ob/ob mice. Among 327 differentially expressed mouse cilia genes, 81 human orthologs are also affected in islets of diabetic donors. Islets of nondiabetic mice and humans show a substantial overlap of upregulated cilia genes that are linked to cell-cycle progression. The shRNA-mediated suppression of KIF3A, essential for ciliogenesis, impairs division of MIN6 beta cells as well as in dispersed primary mouse and human islet cells, as shown by decreased BrdU incorporation. These findings demonstrate the substantial role of cilia-gene regulation on islet function and T2D risk.

INTRODUCTION

Type 2 diabetes (T2D) in combination with obesity constitutes one of the most severe global health threats of our time. It is characterized by beta-cell failure and the inability to compensate for insulin resistance (DeFronzo, 2010). Consistently, in people and mice, genetics are heavily linked to the susceptibility of T2D and obesity. The New Zealand Obese (NZO) mouse represents a model for polygenic T2D and obesity that closely resembles the human disease (Joost and Schürmann, 2014). Recently, we discovered a number of quantitative trait loci (QTL) that participate in obesity and insulin resistance in NZO mice (Chadt et al., 2008; Schallschmidt et al., 2018; Scherneck et al., 2009;

Vogel et al., 2009, 2018) and, furthermore, identified some of the causal disease genes and their specific metabolic effects (e.g., *Zfp69* and *Ifi202b*) (Chung et al., 2015; Stadion et al., 2018). In contrast, the C57BL/6 mouse, which lacks leptin, the B6.V-*Lep^{ob/ob}* (B6-ob/ob) mouse develops severe obesity but is protected from diabetes by an adaptive beta-cell proliferation (Kleinert et al., 2018). By analyzing the islet expression profile of NZO and B6-ob/ob mice, four genes were identified that induce (*Lefty1*, *Pcp4l1*, and *Apoa2*) or inhibit (*Ifi202b*) beta-cell proliferation in the B6-ob/ob mouse (Kluth et al., 2015).

Primary cilia are cellular organelles consisting of a microtubular axoneme that is sheathed by a specialized membrane and anchored by the basal body. Ciliogenesis is initiated by the docking of a centrosome and a ciliary vesicle to the plasma membrane and is followed by extension of the microtubule doublets of the mother centriole (Verti et al., 2015). Maintenance of primary cilia is mediated by a bidirectional, intraflagellar transport system (IFT) (Madhivanan and Aguilar, 2014; Spasic and Jacobs, 2017). Mutations in components of the cilia-centrosome complex have been linked to a group of human diseases termed “ciliopathies” (Hildebrandt et al., 2011). A subset of ciliopathies including Bardet-Biedl syndrome (BBS) and Alström syndrome (ALMS) show metabolic abnormalities, including truncal obesity and greater susceptibility to diabetes (Volta and Gerdes, 2017). In the pancreas, cilia are present in duct and centroacinar cells, as well as in endocrine alpha, beta, and delta cells (Lodh et al., 2014). We recently reported on the role of cilia and basal body proteins in insulin signaling, insulin secretion, and beta-cell function (Gerdes et al., 2014). In addition, *alms* and *bbs* morphant zebrafish show aberrant beta-cell production both at 48 h and at 5 days after fertilization (Lodh et al., 2016). Deletion of core cilia components in the developing pancreas has been linked to ductal cysts, but little is known about the implication of cilia in cell-cycle regulation and cell proliferation of the endocrine pancreas. Moreover, the potential role of cilia genes in diabetes susceptibility is incompletely understood.

Therefore, our aim was to investigate ciliation and cilia-gene expression patterns in islets of obese diabetes-prone NZO



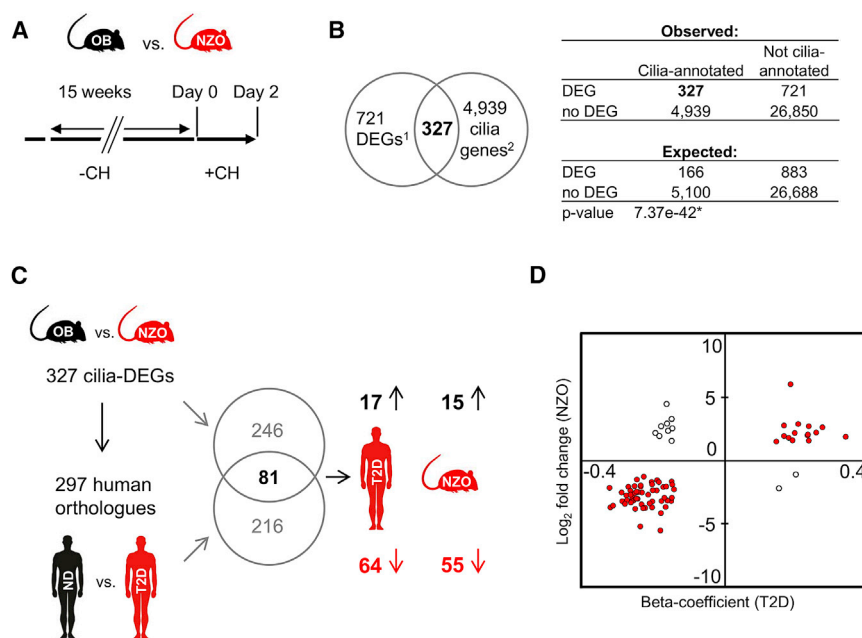


Figure 1. Differentially Expressed Cilia-Annotated Genes in Pancreatic Islets of Diabetes-Resistant B6-ob/ob and Diabetes-Prone NZO Mice Are Also Altered in Human Islets of Diabetic Donors

(A) Experimental setup. Male B6-ob/ob (OB) and NZO mice were fed a carbohydrate-free (–CH), fat-enriched diet until the age of 18 ± 1 week, followed by a diabetogenic food challenge with a carbohydrate-containing diet (+CH) for 2 days. Islet transcriptomics (DNA-microarray) were performed on days 0 and 2, with 3 mice per group.

(B) After 2 days of +CH feeding, 1,048 genes were differentially expressed (DEGs) between B6-ob/ob and NZO islets. (Left) The overlap of those genes with 5,266 orthologs of cilia-annotated genes from the database ²Cilddb for the species *M. musculus*, *R. norvegicus*, and *H. sapiens* (¹ENSEMBL-ID, log₂FC > |1.5|; p < 0.05; n = 3) resulted in 327 differentially expressed cilia genes. (Right) The calculation of a significant enrichment of cilia genes among the DEGs. Depicted are the distributions of genes with and without cilia annotation among the DEGs and non-DEGs (top) and after a permutation analysis with random gene lists (bottom). Expected values

were calculated with 100,000 permutations, including all 32,837 measured transcripts. *p < 0.05; χ^2 -test.

(C) The regulation of the 327 DEGs in OB versus NZO islets upon a 2-day carbohydrate challenge was compared with the regulation of 297 human orthologs between nondiabetic (ND) and diabetic (T2D) donors; 81 human orthologs of differentially expressed mouse cilia genes were associated with T2D in human islets. Of those, 64 genes showed a negative correlation to T2D; of which, 55 genes were also less expressed in islets of diabetes-prone NZO mice; 17 genes were positively correlated to T2D in humans; of which, 15 genes were also upregulated in NZO islets.

(D) The diagram shows the regulation of the 81 overlapping genes in islets of diabetes-prone NZO mice and T2D donors. Negative log₂-fold changes in NZO (y axis) and negative beta coefficients in T2D donors (x axis) represent downregulation in both and vice versa, respectively (red dots). Empty circles represent genes without a coinciding regulation in mice and human.

mice compared with diabetes-resistant B6-ob/ob mice and to screen for similarities in human islets of diabetic versus nondiabetic donors.

RESULTS

Cilia-Annotated Genes Exhibit a Differential Expression in Islets of Diabetes-Prone versus Diabetes-Resistant Mice

Obese B6-ob/ob and NZO mice exhibit different diabetes susceptibilities because of their genetic backgrounds. By use of a special dietary regimen comprising long-term carbohydrate restriction (–CH) and a subsequent carbohydrate intervention (+CH; Figure 1A), we induced hyperglycemia and beta-cell apoptosis in a fast and synchronized manner in NZO animals. Conversely, B6-ob/ob mice compensated for diabetes development with massive islet hyperplasia (Kluth et al., 2015). To test whether both strains differed in expression of cilia-annotated genes, we performed DNA microarray-based transcriptomics of islets from B6-ob/ob and NZO mice after 2 days of carbohydrate intervention and focused on 5,266 genes listed in the database Cilddb (Arnaiz et al., 2014) as related to cilia. We detected 1,048 differentially expressed genes (DEGs; log₂-fold change [log₂FC] > |1.5|; p < 0.05, which corresponds to more than 2.8-fold upregulation or downregulation) in B6-ob/ob and NZO islets, of which 327 are annotated cilia genes (Figure 1B, left); 164 cilia

genes were more abundant in B6-ob/ob mice, and 163 genes were more abundant in NZO islets (Table S1). To uncover a significant enrichment of DEGs with annotations to cilia function, permutation analysis and χ^2 tests were performed with random gene lists of 1,048 genes. We calculated strikingly fewer (n = 166) cilia genes among the random gene list, pointing toward significant (p = 7.37 × 10^{–42}) enrichment of differentially expressed cilia genes in islets of diabetes-resistant B6-ob/ob mice as compared with the diabetes-prone NZO strain (Figure 1B, right).

Islet Cilia-Gene Expression Is Similar in the Diabetic State of Mice and Humans

We next tested whether the detected differentially expressed cilia genes in mice were also affected in human islets of nondiabetic, versus diabetic, donors. RNA-seq-based expression data from the 297 human orthologs of the 327 mouse cilia genes were obtained from an islet cohort of 213 human donors (Table 1) and were used for regression analysis. In total, 81 cilia genes that were differentially expressed in islets of B6-ob/ob and NZO mice significantly correlated to diabetes development in nondiabetic, versus diabetic, human donors (Figure 1C). Interestingly, most of these genes (64) were negatively correlated, and only 17 were positively correlated with T2D in humans. A similar pattern of regulation was detected in the diabetes-prone NZO mouse, in which 55 of the 64 genes were less abundant, and 15 of the 17

Table 1. Detailed Information on Human Islet Donors

Human Donor	Age	BMI	Hba1c	Sex
Nondiabetics	58.5 ± 10.0	26.3 ± 3.8	5.8 ± 0.6	67 females, 103 males
T2D	61.0 ± 10.1	27.9 ± 4.5	6.8 ± 0.9	11 females, 21 males

Means ± SD.

genes were in greater abundance (Figure 1D). Taken together, 70 cilia genes showed similar regulation in islets of diabetes-prone NZO mice and diabetic donors (Figure 1D, red dots). A complete list of the 81 altered cilia genes regulated in both species is provided in Table S2. Collectively, these results show a similar regulation of cilia genes in islets of mice and humans with T2D.

Differentially Expressed Cilia Genes Can Be Linked to Cell-Division Pathways

To clarify in which pathways the 327 differentially expressed mouse cilia genes are involved, Gene Ontology (GO) term-enrichment analysis was performed (Eden et al., 2009). A circular visualization of the mainly enriched processes in B6-ob/ob islets is depicted in Figure 2A, which indicates the regulation of the involved genes and the enrichment score. Decreased terms in B6-ob/ob correspond to increased terms in NZO. The ranking of affected pathways clearly underlines cell division in B6-ob/ob islets as the most probable consequence of altered cilia-gene expression, whereas, in NZO islets, affected cilia genes are involved in the regulation of the extracellular matrix and lipid metabolism (Figure 2A; for detailed information on genes within the pathways, see Tables S3). Figure 2B illustrates the ranked visualization of the mainly enriched GO terms of upregulated cilia genes in B6-ob/ob and NZO islets.

Fewer Cilia in Islets of Diabetes-Prone NZO Mice Associates with Lower Rate of Proliferation

Next, we evaluated the presence of cilia in B6-ob/ob and NZO islets and performed immunohistochemical staining of cilia by detecting acetylated α -tubulin—the most-common, specific cilium marker—in pancreatic sections of B6-ob/ob and NZO mice. NZO islets exhibited fewer cilia compared with B6-ob/ob islets under –CH conditions (Figure 3A, right). After the 2-day +CH intervention, the ciliation of islet cells in NZO mice did not change, whereas B6-ob/ob islets showed a marked reduction in cilia per nuclei (Figure 3A, left). The morphometric analysis confirmed that NZO islets exhibited no alterations in cilia number between –CH and +CH feeding, whereas B6-ob/ob islets displayed more cilia than NZO did, which, significantly, disappeared upon the 2-day +CH challenge (Figure 3B). To evaluate whether the carbohydrate-mediated cilia disassembly occurred in alpha and beta cells, we co-stained pancreas sections of B6-ob/ob mice for acetylated α -tubulin and insulin or glucagon. Cilia are expressed on alpha and beta cells, and their number decreased in both cell types in response to carbohydrate feeding (Figures S1A and S1B). Of note, α -tubulin acetylation is also present in neuronal structures, making absolute quantification difficult. We, therefore,

performed an additional analysis. Isolated islets were fixed and stained for the cilia-specific marker ARL13B (ADP ribosylation factor 13b) and quantified based on the fluorescent signal in intact islets (Figure S1C). These data confirmed that ciliation in NZO islets was reduced by more than 3-fold in comparison with B6-ob/ob islets.

As shown in Figure 3C, islets of B6-ob/ob and NZO mice that were kept under –CH conditions exhibited only a few Ki-67⁺ cells, reflecting proliferating cells. As expected from our earlier observations (Kluth et al., 2015), B6-ob/ob islets exhibited a significant increase in adaptive beta-cell proliferation in response to the 2-day +CH, whereas NZO islets did not (Figure 3C, top), as demonstrated by morphometric analysis (Figure 3C, bottom). Hence, cilia disassembly of islet cells from B6-ob/ob mice is accompanied by an induction of beta-cell proliferation. To detect apoptotic cells, we performed TUNEL assays on pancreatic sections of B6-ob/ob and NZO mice before and 2, 4, 8, and 16 days after carbohydrate feeding (Figure 3D, top). In contrast to B6-ob/ob islets, which did not exhibit any apoptotic cell, NZO islets displayed 0.28% and 0.68% TUNEL-positive cells after 8 and 16 days of carbohydrate feeding, respectively (Figure 3D, bottom).

Differences in Insulin Secretion in B6-ob/ob and NZO Islets

As described previously (Kluth et al., 2014), B6-ob/ob mice transiently increase their blood glucose levels shortly after the switch from a –CH to a +CH diet and return to normoglycemia afterward. In contrast, blood glucose concentration increased continuously in NZO mice (Figure 4A). To characterize the islet function of B6-ob/ob and NZO mice, we isolated their islets before and 2 days after +CH feeding (at the same times that expression profiles and cilia were analyzed) and evaluated the glucose-mediated insulin secretion. Body weights of the four groups were not different (Figure 4B). Figure 4C shows the blood glucose concentrations and plasma insulin values of mice that were used for islet isolation and detection of insulin secretion. After 2 days of +CH feeding, blood glucose levels did not increase significantly in B6-ob/ob, but did increase in NZO mice; plasma insulin levels were elevated in both mouse strains. Perfusion experiments under low (2.8 mmol/L) and high (20 mmol/L) glucose revealed no significant differences in insulin secretion between NZO and B6-ob/ob islets on –CH feeding (Figures 4D, left, and 4E); the latter secrete moderately, but not significantly, less insulin. Two days after the diet switch (+CH), B6-ob/ob islets responded normally, first, with increased insulin secretion at 20 mmol/L glucose, followed by a drop of insulin secretion in response to 2.8 mmol/L glucose (Figures 4D, right, and 4E). In contrast, islets of NZO mice appeared to be less flexible; they exhibited significantly elevated, glucose-mediated first and second phases of insulin secretion and did not reduce the release of insulin appropriately at 2.8 mmol/L glucose.

Islets of B6-ob/ob Mice and Non-diabetic Humans Exhibit Higher Expression Levels of Cilia Genes Involved in Cell Cycle

As shown above, cilia retraction and induction of proliferation in islets of B6-ob/ob mice occurred in response to the carbohydrate

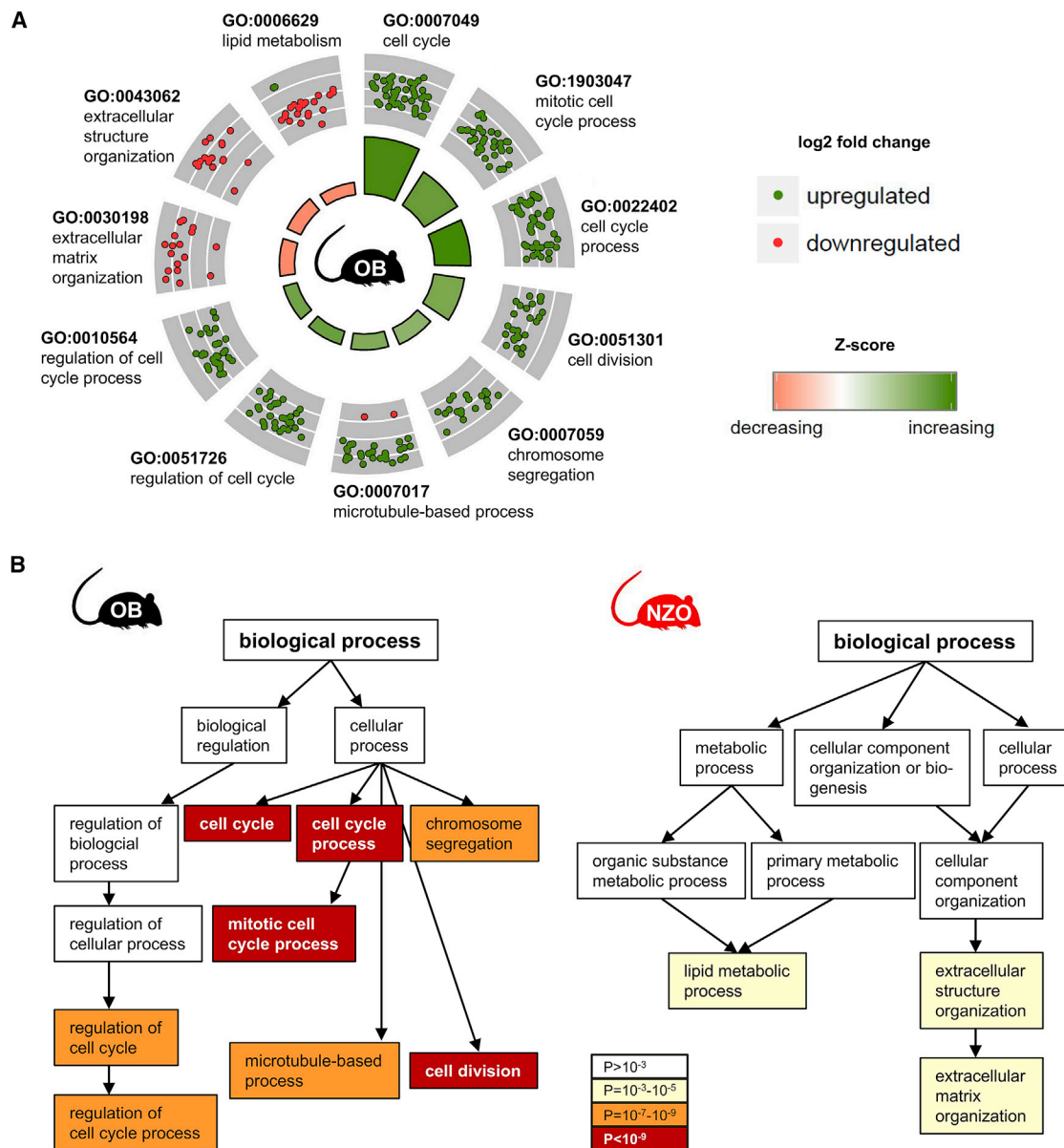


Figure 2. Upregulated Islet Cilia Genes in Diabetes-Resistant B6-ob/ob Mice Are Mainly Involved in Cell-Division Processes

(A) Circular visualization of gene-annotation enrichment analysis (GOcircle) with the 327 differentially regulated cilia genes in B6-ob/ob (OB) versus NZO islets. The inner circle depicts the main processes to be increased (green) or decreased (red) in OB islets. The outer circle shows scaled scatter plots for involved genes and their regulation within the most-enriched biological processes (GO term). The more outside the dots are located, the lower is their p value of regulation. Red dots mark downregulated, and green dots mark upregulated genes in OB islets (\log_2FC). The Z score (inner circle) defines the likelihood of a process being decreased (red) or increased (green) in OB islets.

(B) Ranked visualization of the mainly enriched GO terms by upregulated cilia genes in B6-ob/ob and NZO islets. p values for enrichment are $<10^{-7}$ (B6-ob/ob) and $<10^{-4}$ (NZO).

challenge. This prompted us to test whether the 81 cilia genes detected in mice and humans were specifically induced by the diet. We overlapped those cilia genes that were affected by the diet switch (85 genes in B6-ob/ob islets [Table S4]; 4 genes in NZO islets [Table S4]) with the 81 human differentially expressed cilia genes; 50 of the diet-regulated cilia genes in B6-ob/ob islets were also altered in human islets,

whereas none of the 4 NZO genes overlapped with the human gene list (Figure 5A). Interestingly, 49 of those dual-altered genes were upregulated, and only one gene was repressed in B6-ob/ob islets. Without exception, the cilia-genes showed the same pattern in human islets of nondiabetic donors (Figure 5B). Strikingly, 39 of the 49 diet-induced cilia genes in B6-ob/ob islets could be linked to the cell cycle (Table S4). For

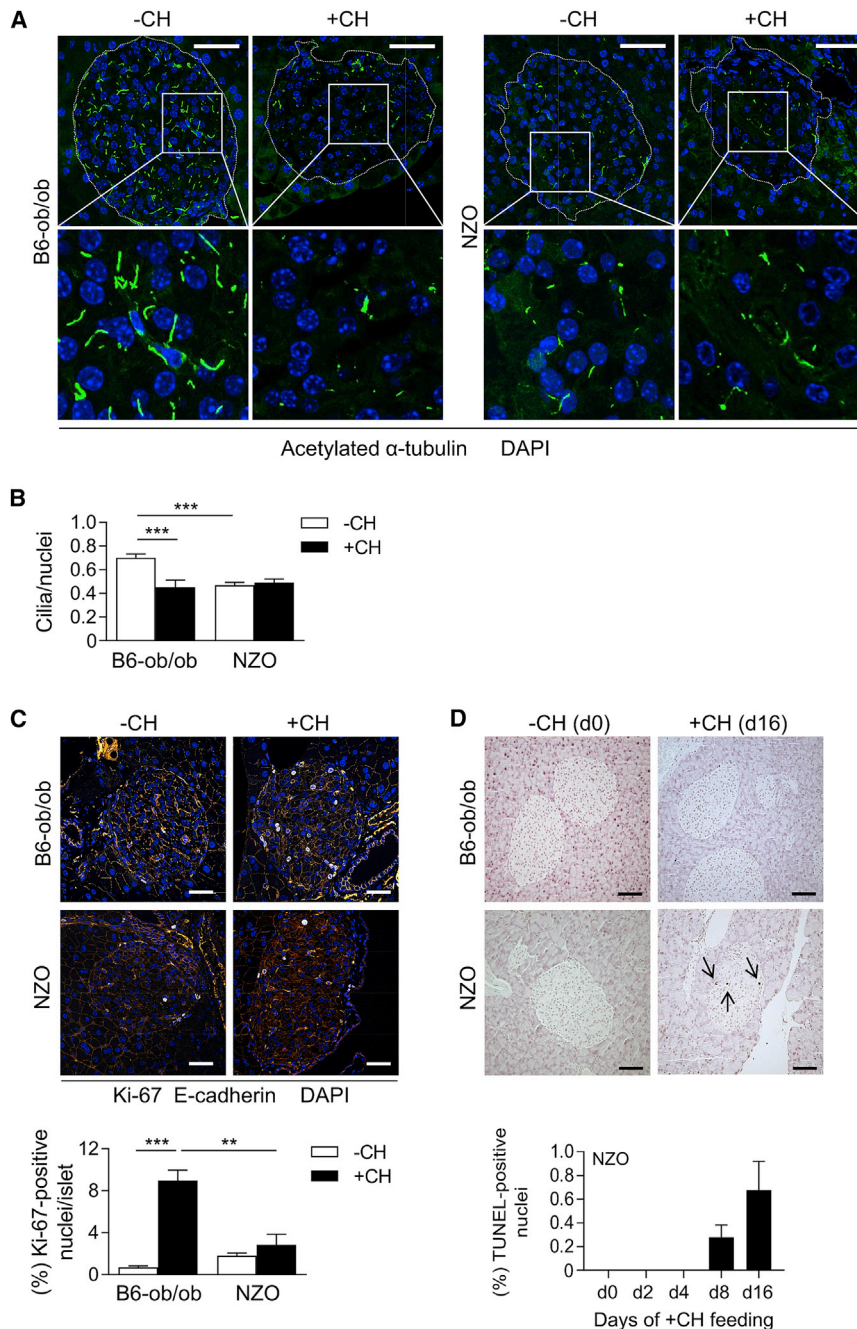


Figure 3. Islets of Diabetes-Resistant B6-ob/ob Mice Exhibit More Cilia Than Those of the Diabetes-Prone NZO Strain

(A) Representative images of pancreatic sections of B6-ob/ob and NZO mice stained for acetylated α -tubulin (green) as a marker of cilia. Samples were taken before carbohydrate feeding (–CH; left) and after 2 days of carbohydrate feeding (+CH; right). Nuclei were stained with DAPI (blue). Scale bars, 50 μ m.

(B) Morphometric analysis of ciliation was performed in randomly selected islets of three to five pancreases per group. Data are means \pm SEM. *** p < 0.001; two-way ANOVA with Sidak's multiple comparisons test.

(C) Representative images of pancreatic islets of carbohydrate-deprived (–CH) or carbohydrate-challenged (+CH) B6-ob/ob and NZO mice stained for the cell proliferation marker Ki-67 with corresponding quantification as determined by the percentage of Ki-67⁺ nuclei to all nuclei. Data are means \pm SEM of randomly selected islets from the pancreases of four to six animals per group. White: Ki-67, blue: nuclei (DAPI), orange: cell membrane (E-cadherin). Scale bars, 50 μ m. ** p < 0.01, *** p < 0.001; two-way ANOVA with Sidak's multiple comparisons test.

(D) Representative images showing TUNEL-positive nuclei (brown, indicated by the arrows) detected in pancreatic islets of B6-ob/ob and NZO mice with corresponding quantification for NZO at indicated times. Scale bars, 50 μ m.

prevent the development of diabetes by maintaining a suitable glucose response.

KIF3A Suppression in MIN6 Beta Cells and Primary Mouse Islet Cells Decreases Their Proliferation Capacity

To test the hypothesis that an appropriate cilia function is required for the induction of proliferation, we screened for a cilia gene that is differentially expressed in islets of B6-ob/ob and NZO mice and, at the same time, is affected in the islets of patients with T2D to suppress its expression and determine cell replication. Because many central cilia genes, such as *Aurka*, the aurora kinase

two representative gene products—alcohol dehydrogenase 1 (ADH1) and hyaluronan-mediated motility receptor (RHAMM, HMMR)—we performed western blot analysis of islet lysates. The results confirmed the findings of the array analysis; ADH1 had fewer and HMMR had a slightly greater abundance in B6-ob/ob islets than in NZO islets (Figure 5C). In summary, cilia-gene induction could be linked to the regulation of beta-cell proliferation and/or to an appropriate regulation of glucose-stimulated insulin secretion. Because human islets have no, or very limited, capacity to proliferate, cilia-gene induction might

A gene, are also directly implicated in proliferation (Fu et al., 2007), we had to identify a candidate that was, rather, involved in cilia organization. We selected *Kif3a*, encoding the kinesin family member 3A, which has been documented as a key factor in ciliogenesis and the intraflagellar transport of primary cilia (Jiang et al., 2016; Rosenbaum and Witman, 2002). Murine *Kif3a* expression was significantly less in NZO, as compared with B6-ob/ob, islets (Figure 6A, left), and KIF3A protein tended to be decreased after high glucose treatment (Figure 6A, right). Similarly, human *KIF3A* mRNA levels were

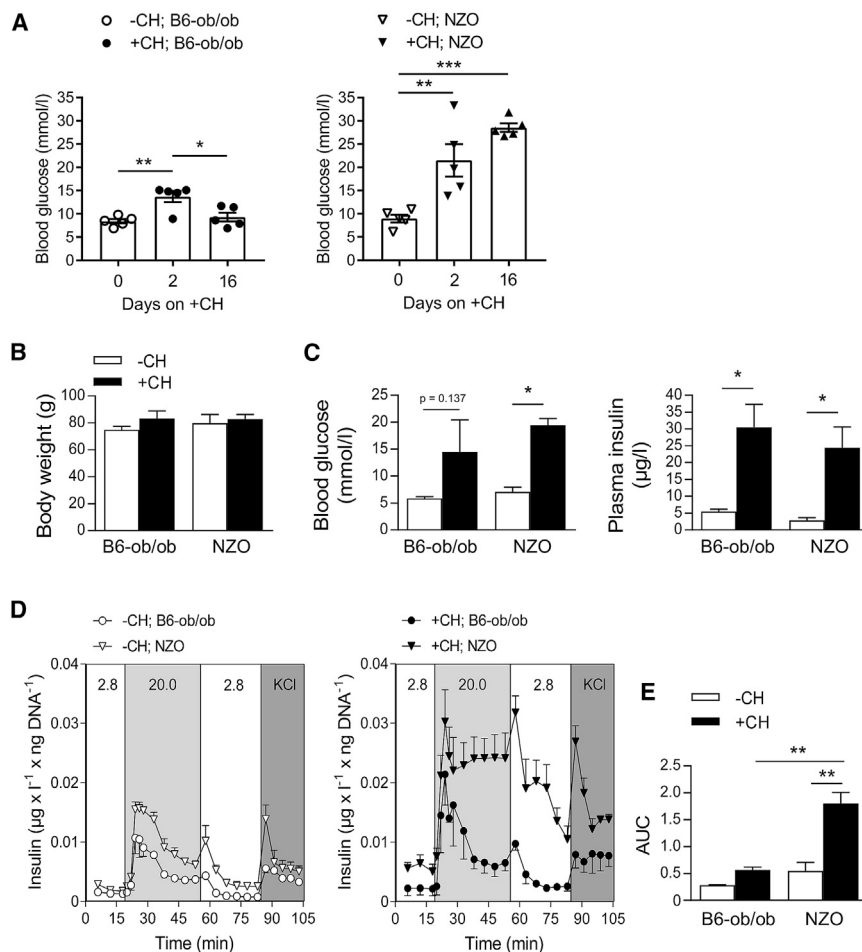


Figure 4. Differences in Glucose-Stimulated Insulin Secretion in B6-ob/ob and NZO Islets Before and After Carbohydrate Feeding

(A) Blood glucose concentrations of B6-ob/ob and NZO mice before (–CH) as well as 2 and 16 days after the intervention with a carbohydrate-containing diet (+CH). Data are means \pm SEM, $n = 5$ animals per mouse strain. * $p < 0.05$, ** $p < 0.01$, *** $p < 0.001$; one-way ANOVA with Tukey's multiple comparisons test.

(B and C) Body weight (B) and blood glucose levels (left; C) and plasma insulin concentrations (right; C) of B6-ob/ob and NZO mice fed either without carbohydrates (–CH) or with a subsequent 2-day carbohydrate challenge (+CH). Data are mean \pm SEM, $n = 3$ to 4 animals per mouse strain, * $p < 0.05$, two-way ANOVA with Sidak's multiple comparisons test.

(D) Glucose-stimulated insulin secretion of freshly isolated B6-ob/ob (circles) and NZO (triangles) islets under –CH (left) or +CH (right) feeding with corresponding area under the curve shown in (E). Data are presented as means \pm SEM, $n = 3$ –4 animals per mouse strain and treatment. ** $p < 0.01$; two-way ANOVA with Sidak's multiple comparisons test.

negatively correlated with elevated hemoglobin A1c (HbA1c) values (Figure 6B). For functional analysis, we used MIN6 cells and infected them with scrambled or *Kif3a*-specific short hairpin RNA (shRNA) adenoviruses. Six days after infection, *Kif3a* mRNA and KIF3A protein levels (Figure 6C) were significantly suppressed in *Kif3a* shRNA-infected cells than they were in control cells (sh-scr). Similar to the protein content of KIF3A, the cilium marker acetylated α -tubulin was markedly reduced (Figure 6C, right) as was the number of cilia per nuclei (Figure 6D). To evaluate the proliferation capacity of control and *Kif3a* shRNA-transfected MIN6 cells, those cells were treated with BrdU for 2 h and were subsequently stained for BrdU. The knockdown of *Kif3a* resulted in significantly decreased BrdU incorporation (Figures 6E and S2), which provides direct functional evidence for the involvement of cilia in beta-cell proliferation. To test whether the suppressed proliferation was mediated by an off-target effect of the *Kif3a*-shRNA, a genetic-rescue experiment was performed. Cells were transfected with the *Kif3a* shRNA plus a plasmid encoding an optimized *Kif3a* sequence, which was translated into the same protein sequence but was not targeted by the *Kif3a*-shRNA (Figure 6F). Although infection with *Kif3a* shRNA reduced the rate of proliferation, rescued cells showed no effect (Figure 6G, right). In contrast,

BrdU and acetylated α -tubulin. Similar to MIN6 cells, primary islet cells exhibited fewer cilia and a lower proliferation rate in *Kif3a*-depleted cells as compared with control cells (Figure 6H). However, suppression of *Kif3a* in primary islet cells did not influence the first and second phases of insulin secretion (Figure S4). Data on dispersed primary human islet cells from two different donors that were infected with control or sh-KIF3A adenovirus and treated with harmine and BrdU (Figure S5C) confirmed that KIF3A silencing reduces islet cell proliferation (by about 60%) (Figure 6I).

DISCUSSION

In the present study, we provide novel data on islet cilia gene regulation and its role in diabetes susceptibility. Particularly, by comparing the expression profiles of cilia-annotated genes in islets of obese mouse models and islets from human donors, we highlight their involvement in beta-cell division and the regulation of glucose-stimulated insulin secretion as a mechanism for preventing diabetes. Our data show that diabetes-resistant B6-ob/ob mice exhibited (1) more cilia that were able to (2) disassemble in response to a dietary carbohydrate challenge, indicating that functional cilia dynamics in islets are essential

the overexpression of *Kif3a* did not affect BrdU incorporation (Figure S3).

To confirm the findings obtained in MIN6 cells, mouse islets were isolated from B6 mice, cells were dispersed, and *Kif3a* expression was downregulated (Figure 6H). Cells were treated with BrdU for 24 h and co-stained against

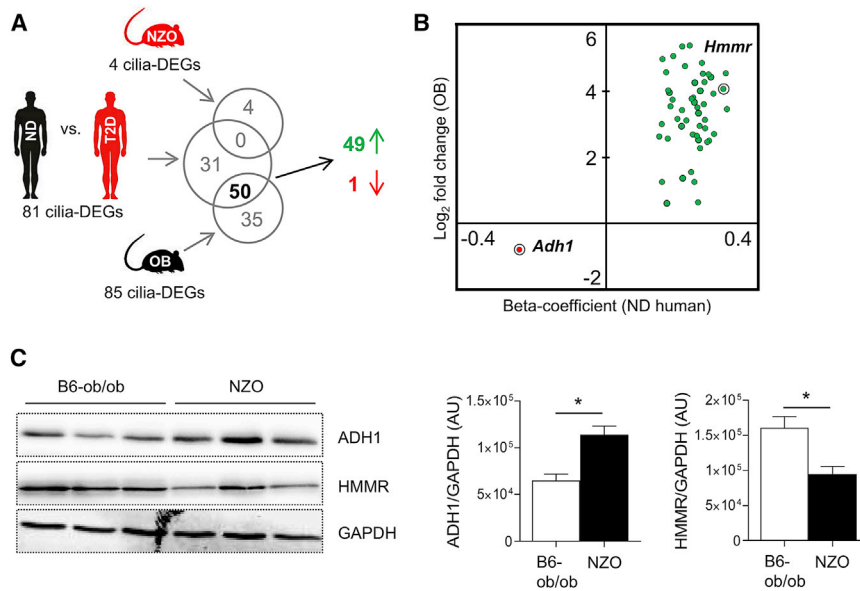


Figure 5. Diet-Activated Cilia Genes in Diabetes-Resistant B6-ob/ob Islets Show Greater Expression in Islets of Nondiabetic Humans

(A) The 81 human cilia genes that are differentially regulated in nondiabetic (ND) versus diabetic (T2D) donors were overlaid with mouse cilia genes that were significantly altered between –CH and +CH feeding (OB: 85 genes, NZO: 4 genes). A huge number of 50 cilia genes regulated in diabetes-resistant OB islets overlaps with human cilia genes that are altered in T2D; 49 of those genes are upregulated in ND and OB, and only one gene, the alcohol dehydrogenase 1 (*Adh1*), is down-regulated.

(B) The diagram shows the regulation of the 50 overlapping genes in OB islets and nondiabetic human donors (ND) as depicted by log₂-fold changes (y axis) and beta coefficients (x axis).

(C) The western blot analysis results of ADH1 and HMMR in islets of B6-ob/ob and NZO mice at the age of 18 weeks with corresponding quantifications (n = 3). Glyceraldehyde 3-phosphate dehydrogenase (GAPDH) was used as a loading control. Data are mean ± SEM, n = 3, *p < 0.05 by Student's t test.

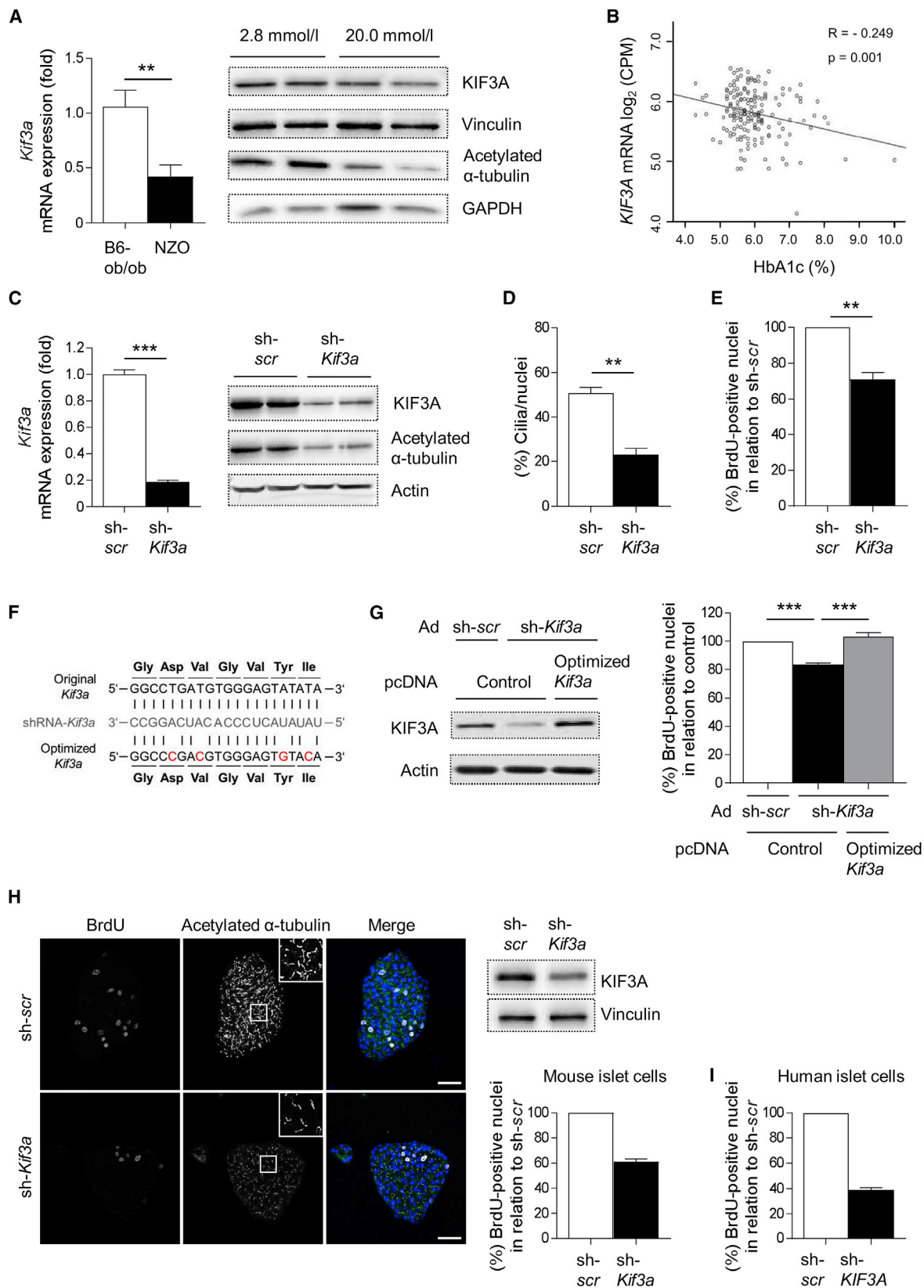
for the induction of beta-cell proliferation and/or for sufficient flexibility of islets to reduce the insulin secretion after the second phase. In fact, suppression of KIF3A, a key factor in ciliogenesis, resulted in a lower proliferation rate in MIN6 and primary mouse and human islet cells but did not affect glucose-stimulated insulin secretion.

The question that remains open is what happens first, the signaling from the cell-cycle machinery that triggers cilia disassembly or signals from the cilium itself that regulate cell-cycle entry? Numerous studies have described the importance of cilia disassembly in a wide variety of cycling cells (Tucker et al., 1979; Goto et al., 2016; Liang et al., 2016; Plotnikova et al., 2009). In response to a 2-day carbohydrate intervention, B6-ob/ob mice exhibit an islet cilia-gene expression profile that mirrors the highly conserved signaling from the cell-cycle machinery provoking cilia disassembly (Korobeynikov et al., 2017). The hypothesis that this effect can be initiated by the cilium itself can be substantiated by the finding of differentially expressed cilia genes that are detected already at a pre-diabetic state (–CH feeding) in B6-ob/ob and NZO islets. Because cilia act as sensory organelles, the lower abundance of cilia in NZO islets may prevent external cues from triggering beta-cell proliferation and the regulation of insulin secretion, for instance, in response to elevated blood glucose levels. Currently, we cannot define how cilia dysfunction is directly linked to diabetes. Beside an impaired induction of cell division and an alteration of first and second phases of insulin secretion, a secretory dysfunction of alpha cells and differences in islet insulin sensitivity and other factors might be involved in determining diabetes susceptibility. Likewise, *BBS* mutations in humans impair cilia/basal body function in a variety of tissues leading to numerous defects, including insulin resistance and T2D (Badano et al., 2006; Novas et al., 2015). In fact, several cilia-mediated paracrine signals, such as Hedgehog, platelet-derived

growth factor receptor alpha (PDGFR α), or Wnt, are described as regulators of proliferation and differentiation (Irigoin and Badano, 2011). Whether misregulated ciliary receptor signaling accounts for the inability of NZO beta cells to proliferate is not currently known and needs further investigation. Interestingly, among the 327 differentially expressed cilia genes, some encoded receptors are altered, of which, for instance, *Folr1* (Necela et al., 2015) or *Cckar* (Rai et al., 2016) are described as being involved in cell division (see Table S1). The *in vitro* suppression of KIF3A, which resulted in a significant reduction of BrdU incorporation, clearly supports the hypothesis that the initial signal for the induction of proliferation is initiated via an appropriate cilia function.

B6-ob/ob and NZO mice showed no differences in their plasma insulin levels shortly after the switch to a carbohydrate-containing diet, whereas at the same time insulin secretion by NZO islets was greater than it was for B6-ob/ob islets. This discrepancy between *in vivo* and *in vitro* data might be explained by differences in the total number and size of islets in the two strains; B6-ob/ob exhibit more and larger islets than NZO mice do (Kluth et al., 2015). However, the fewer cilia in NZO islets and the limited disassembly in response to carbohydrates does not result in a loss of insulin secretion, but rather, in hypersecretion. This effect might be explained by the fact that NZO islet cells do not enter the cell cycle and thereby maintain their insulin secretion at least until the beta cells undergo apoptosis.

Evidence of dysregulated islet cilia genes in connection to diabetes has also been observed in the diabetes-prone Goto-Kakizaki (GK) rat. Beta-cell mass is reduced in GK rats and seems to be linked to both defects in beta-cell proliferation and to de-differentiation, a finding that coincides with NZO islets in the present study. Similar to NZO mice, cilia genes and proteins were misregulated in GK islets (Gerdes et al., 2014).



(legend on next page)

In conclusion, our data support cilia-gene regulation as having a strong impact on the presence and dynamics of cilia in islets, which, in turn, determines diabetes susceptibility.

STAR★METHODS

Detailed methods are provided in the online version of this paper and include the following:

- KEY RESOURCES TABLE
- CONTACT FOR REAGENT AND RESOURCE SHARING
- EXPERIMENTAL MODEL AND SUBJECT DETAILS
 - Animals
 - Cell lines
 - Adenoviruses
 - Human islets
- METHOD DETAILS
 - Isolation of pancreatic islets and transcriptome analysis
 - Glucose-stimulated insulin secretion in primary mouse islets
 - Histological and immunofluorescence staining of pancreatic sections and morphometry
 - Whole mount staining of murine islets and morphometry
 - Cell culture, transfection and BrdU assay in MIN6 and primary mouse and human islet cells
 - Western Blot analysis
 - Human islet RNA sequencing
- QUANTIFICATION AND STATISTICAL ANALYSIS
- DATA AND SOFTWARE AVAILABILITY

SUPPLEMENTAL INFORMATION

Supplemental Information can be found with this article online at <https://doi.org/10.1016/j.celrep.2019.02.056>.

ACKNOWLEDGMENTS

The study was supported by grants from the German Ministry of Education and Research (BMBF: DZD grant 82DZD00302), the State of Brandenburg, the

German Diabetes Association (DDG: common project funding from 2017/02/21), the German Research Foundation (DFG; SFB-958), the Swedish Research Council, Novo Nordisk Foundation, and Linné grant (B31 5631/2006, Exodiab, SSF and Region Skåne). The funders had no role in the study design, data collection and analysis, decision to publish, or preparation of the manuscript. Human islets were provided through the JDRF award 31-2008-416 (ECIT Islet for Basic Research program) and the EXODIAB Human Tissue Lab, Lund University. We kindly thank A. Pfeifer of the University of Bonn (Germany) for discussions on this manuscript. The skillful technical assistance of Sarah Ernst, Anett Helms, and Juliane Egert is gratefully acknowledged.

AUTHOR CONTRIBUTIONS

O.K., A. Schürmann, and C.L. conceived and designed the experiments. O.K., M.S., P.G., H.A., M.J., S.S., H.V., U.K., A. Seelig, C.L., and J.G. contributed to the acquisition and analysis of data. O.K., A. Schürmann, M.S., C.L., and J.G. participated in the drafting and writing of the manuscript. A. Schürmann, O.K., M.S., H.V., U.K., C.L., and J.G. were responsible for critical revision of the manuscript. All authors contributed to the interpretation of data, editing of the manuscript, and approval of its final version for publication. A. Schürmann is the guarantor of this work.

DECLARATION OF INTERESTS

The authors declare no competing interests.

Received: April 11, 2018

Revised: December 21, 2018

Accepted: February 14, 2019

Published: March 12, 2019

REFERENCES

- Arnaiz, O., Malinowska, A., Klotz, C., Sperling, L., Dadlez, M., Koli, F., and Cohen, J. (2009). Cildb: a knowledgebase for centrosomes and cilia. *Database (Oxford)* 2009, bap022.
- Arnaiz, O., Cohen, J., Tassin, A.M., and Koli, F. (2014). Remodeling Cildb, a popular database for cilia and links for ciliopathies. *Cilia* 3, 9.
- Badano, J.L., Mitsuma, N., Beales, P.L., and Katsanis, N. (2006). The ciliopathies: an emerging class of human genetic disorders. *Annu. Rev. Genomics Hum. Genet.* 7, 125–148.
- Chadt, A., Leicht, K., Deshmukh, A., Jiang, L.Q., Scherneck, S., Bernhardt, U., Dreja, T., Vogel, H., Schmolz, K., Kluge, R., et al. (2008). *Tbc1d1* mutation in lean mouse strain confers leanness and protects from diet-induced obesity. *Nat. Genet.* 40, 1354–1359.

Figure 6. Suppression of KIF3A in MIN6 and Primary Mouse and Human Islet Cells Inhibits Cell Replication

(A) *Kif3a* mRNA expression in pancreatic islets of diabetes-resistant B6-ob/ob and diabetes-prone NZO mice and western blot analysis of KIF3A and acetylated α -tubulin in B6 islets treated with either 2.8 or 20 mmol/L glucose for 24 h. Data are shown as means \pm SEM of three animals per mouse strain. ** $p < 0.01$ by Student's *t* test.

(B) Correlation of *Kif3a* mRNA levels in human pancreatic islets with plasma HbA1c values of 170 nondiabetic and 32 diabetic donors ($R^2 = 0.062$).

(C) MIN6 beta cells were transfected with adenoviruses encoding *Kif3a*-specific shRNA to suppress KIF3A expression. Scrambled shRNA-encoding adenoviruses were used as a control (sh-scr). Five days after transfection, cells were harvested for mRNA (left) or protein (right) analysis. Actin was used as a loading control. Data are depicted as means \pm SEM, $n = 4$. *** $p < 0.001$ by Student's *t* test.

(D) Number of cilia per nuclei in control and KIF3A-depleted cells.

(E) Quantification of BrdU⁺ nuclei per total number of nuclei in MIN6 cells after 2 h of BrdU incubation. Data are means \pm SEM of three independent experiments. ** $p < 0.01$ by Student's *t* test.

(F) Sequences of the *Kif3a*-specific shRNA, wild-type, and the optimized *Kif3a* RNA used for the rescue experiment.

(G) The western blot (left) and BrdU incorporation (right) analysis after KIF3A suppression and genetic rescue. Data are means \pm SEM of three independent experiments. *** $p < 0.001$ by Student's *t* test.

(H) Representative fluorescence images showing BrdU⁺ nuclei and cilia (acetylated α -tubulin) in dispersed primary mouse islets transfected with control (sh-scr; top) or *Kif3a*-specific (sh-*Kif3a*; bottom) adenoviruses with respective quantification for BrdU⁺ nuclei and KIF3A suppression, as detected by western blot analysis. Vinculin was used as a loading control. Data are means \pm SEM of two independent experiments. Scale bars, 50 μ m.

(I) Quantification of BrdU⁺ nuclei per total number of nuclei in dispersed primary human islet cells transfected with control (sh-scr) or *Kif3a*-specific (sh-*KIF3A*) adenoviruses after 4 days of harmine (10 μ mol/L) and BrdU treatment. Data are means \pm SEM of two independent experiments.

- Chung, B., Stadion, M., Schulz, N., Jain, D., Scherneck, S., Joost, H.G., and Schürmann, A. (2015). The diabetes gene *Zfp69* modulates hepatic insulin sensitivity in mice. *Diabetologia* 58, 2403–2413.
- DeFronzo, R.A. (2010). Insulin resistance, lipotoxicity, type 2 diabetes and atherosclerosis: the missing links. The Claude Bernard Lecture 2009. *Diabetologia* 53, 1270–1287.
- Eden, E., Navon, R., Steinfeld, I., Lipson, D., and Yakhini, Z. (2009). GOrilla: a tool for discovery and visualization of enriched GO terms in ranked gene lists. *BMC Bioinformatics* 10, 48.
- Fu, J., Bian, M., Jiang, Q., and Zhang, C. (2007). Roles of Aurora kinases in mitosis and tumorigenesis. *Mol. Cancer Res.* 5, 1–10.
- Gerdas, J.M., Christou-Savina, S., Xiong, Y., Moede, T., Moruzzi, N., Karlsson-Edlund, P., Leibiger, B., Leibiger, I.B., Östenson, C.-G., Beales, P.L., and Berggren, P.O. (2014). Ciliary dysfunction impairs beta-cell insulin secretion and promotes development of type 2 diabetes in rodents. *Nat. Commun.* 5, 5308.
- Goto, H., Inaba, H., and Inagaki, M. (2016). Mechanisms of ciliogenesis suppression in dividing cells. *Cell. Mol. Life Sci.* 74, 881–890.
- Hildebrandt, F., Benzing, T., and Katsanis, N. (2011). Ciliopathies. *N. Engl. J. Med.* 364, 1533–1543.
- Irigoin, F., and Badano, J.L. (2011). Keeping the balance between proliferation and differentiation: the primary cilium. *Curr. Genomics* 12, 285–297.
- Jiang, S., Chen, G., Feng, L., Jiang, Z., Yu, M., Bao, J., and Tian, W. (2016). Disruption of *kif3a* results in defective osteoblastic differentiation in dental mesenchymal stem/precursor cells via the Wnt signaling pathway. *Mol. Med. Rep.* 14, 1891–1900.
- Joost, H.-G., and Schürmann, A. (2014). The genetic basis of obesity-associated type 2 diabetes (diabesity) in polygenic mouse models. *Mamm. Genome* 25, 401–412.
- Kleinert, M., Clemmensen, C., Hofmann, S.M., Moore, M.C., Renner, S., Woods, S.C., Huypens, P., Beckers, J., de Angelis, M.H., Schürmann, A., et al. (2018). Animal models of obesity and diabetes mellitus. *Nat. Rev. Endocrinol.* 14, 140–162.
- Kluth, O., Mirhashemi, F., Scherneck, S., Kaiser, D., Kluge, R., Neschen, S., Joost, H.G., and Schürmann, A. (2011). Dissociation of lipotoxicity and glucotoxicity in a mouse model of obesity associated diabetes: role of forkhead box O1 (FOXO1) in glucose-induced beta cell failure. *Diabetologia* 54, 605–616.
- Kluth, O., Matzke, D., Schulze, G., Schwenk, R.W., Joost, H.-G., and Schürmann, A. (2014). Differential transcriptome analysis of diabetes-resistant and -sensitive mouse islets reveals significant overlap with human diabetes susceptibility genes. *Diabetes* 63, 4230–4238.
- Kluth, O., Matzke, D., Kamitz, A., Jähnert, M., Vogel, H., Scherneck, S., Schulze, M., Staiger, H., Machicao, F., Häring, H.U., et al. (2015). Identification of four mouse diabetes candidate genes altering β -cell proliferation. *PLoS Genet.* 11, e1005506.
- Korobeynikov, V., Deneka, A.Y., and Golemis, E.A. (2017). Mechanisms for nonmitotic activation of Aurora-A at cilia. *Biochem. Soc. Trans.* 45, 37–49.
- Liang, Y., Meng, D., Zhu, B., and Pan, J. (2016). Mechanism of ciliary disassembly. *Cell. Mol. Life Sci.* 73, 1787–1802.
- Lodh, S., O'Hare, E.A., and Zaghloul, N.A. (2014). Primary cilia in pancreatic development and disease. *Birth Defects Res. C Embryo Today* 102, 139–158.
- Lodh, S., Hostelley, T.L., Leitch, C.C., O'Hare, E.A., and Zaghloul, N.A. (2016). Differential effects on β -cell mass by disruption of Bardet-Biedl syndrome or Alstrom syndrome genes. *Hum. Mol. Genet.* 25, 57–68.
- Madhivanan, K., and Aguilar, R.C. (2014). Ciliopathies: the trafficking connection. *Traffic* 15, 1031–1056.
- Necela, B.M., Crozier, J.A., Andorfer, C.A., Lewis-Tuffin, L., Kachergus, J.M., Geiger, X.J., Kalari, K.R., Serie, D.J., Sun, Z., Moreno-Aspitia, A., et al. (2015). Folate receptor- α (FOLR1) expression and function in triple negative tumors. *PLoS ONE* 10, e0122209.
- Novas, R., Cardenas-Rodriguez, M., Irigoín, F., and Badano, J.L. (2015). Bardet-Biedl syndrome: Is it only cilia dysfunction? *FEBS Lett.* 589, 3479–3491.
- Ottosson-Laakso, E., Krus, U., Storm, P., Prasad, R.B., Oskolkov, N., Ahlqvist, E., Fadista, J., Hansson, O., Groop, L., and Vikman, P. (2017). Glucose-induced changes in gene expression in human pancreatic islets: causes or consequences of chronic hyperglycemia. *Diabetes* 66, 3013–3028.
- Plotnikova, O.V., Pugacheva, E.N., and Golemis, E.A. (2009). Primary cilia and the cell cycle. *Methods Cell Biol.* 94, 137–160.
- Rai, R., Kim, J.J., Tewari, M., and Shukla, H.S. (2016). Heterogeneous expression of cholecystokinin and gastrin receptor in stomach and pancreatic cancer: an immunohistochemical study. *J. Cancer Res. Ther.* 12, 411–416.
- Rodriguez-Diaz, R., Abdulreda, M.H., Formoso, A.L., Gans, I., Ricordi, C., Berggren, P.O., and Caicedo, A. (2011). Innervation patterns of autonomic axons in the human endocrine pancreas. *Cell Metab.* 14, 45–54.
- Rosenbaum, J.L., and Witman, G.B. (2002). Intraflagellar transport. *Nat. Rev. Mol. Cell Biol.* 3, 813–825.
- Schallschmidt, T., Lebek, S., Altenhofen, D., Damen, M., Schulte, Y., Knebel, B., Herwig, R., Rasche, A., Stermann, T., Kamitz, A., et al. (2018). Two novel candidate genes for insulin secretion identified by comparative genomics of multiple backcross mouse populations. *Genetics* 210, 1527–1542.
- Scherneck, S., Nestler, M., Vogel, H., Blüher, M., Block, M.-D., Berriel Diaz, M., Herzog, S., Schulz, N., Teichert, M., Tischer, S., et al. (2009). Positional cloning of zinc finger domain transcription factor *Zfp69*, a candidate gene for obesity-associated diabetes contributed by mouse locus *Nidd/SJL*. *PLoS Genet.* 5, e1000541.
- Spasic, M., and Jacobs, C.R. (2017). Primary cilia: cell and molecular mechanosensors directing whole tissue function. *Semin. Cell Dev. Biol.* 71, 42–52.
- Stadion, M., Schwerbel, K., Graja, A., Baumeier, C., Rödiger, M., Jonas, W., Wolfrum, C., Staiger, H., Fritsche, A., Häring, H.-U., et al. (2018). Increased *Irf202b/IFI16* expression stimulates adipogenesis in mice and humans. *Diabetologia* 61, 1167–1179.
- R Core Team (2017). R: a language and environment for statistical computing (R Foundation for Statistical Computing).
- Tucker, R.W., Pardee, A.B., and Fujiwara, K. (1979). Centriole ciliation is related to quiescence and DNA synthesis in 3T3 cells. *Cell* 17, 527–535.
- Vertii, A., Bright, A., Delaval, B., Hehnly, H., and Doxsey, S. (2015). New frontiers: discovering cilia-independent functions of cilia proteins. *EMBO Rep.* 16, 1275–1287.
- Vogel, H., Nestler, M., Rüschendorf, F., Block, M.D., Tischer, S., Kluge, R., Schürmann, A., Joost, H.G., and Scherneck, S. (2009). Characterization of *Nob3*, a major quantitative trait locus for obesity and hyperglycemia on mouse chromosome 1. *Physiol. Genomics* 38, 226–232.
- Vogel, H., Kamitz, A., Hallahan, N., Lebek, S., Schallschmidt, T., Jonas, W., Jähnert, M., Gottmann, P., Zellner, L., Kanzleiter, T., et al. (2018). A collective diabetes cross in combination with a computational framework to dissect the genetics of human obesity and type 2 diabetes. *Hum. Mol. Genet.* 27, 3099–3112.
- Volta, F., and Gerdas, J.M. (2017). The role of primary cilia in obesity and diabetes. *Ann. NY Acad. Sci.* 1391, 71–84.
- Walter, W., Sánchez-Cabo, F., and Ricote, M. (2015). GOrilla: an R package for visually combining expression data with functional analysis. *Bioinformatics* 31, 2912–2914.

STAR★METHODS

KEY RESOURCES TABLE

REAGENT OR RESOURCE	SOURCE	IDENTIFIER
Antibodies		
acetylated α -tubulin	Sigma	Cat# T6793; RRID:AB_477585
E-Cadherin	BD Bioscience	Cat# 610181; RRID:AB_397580
Ki-67	Abcam	Cat#ab155580; RRID:AB_443209
Arl13b	Proteintech	Cat# 17711-1-AP; RRID:AB_2060867
BrdU	Sigma	Cat# B8434; RRID:AB_476811
Kif3a	Abcam	Cat# ab11259; RRID:AB_297878
Adh1	Cell Signaling	Cat# 5295; RRID:AB_10626624
Hmmr	MyBioSource	Cat#MBS126929; RRID:AB_2783854
GAPDH	Thermo Fisher Scientific	Cat# AM4300; RRID:AB_2536381
Vinculin	Santa Cruz	Cat# sc-73614; RRID:AB_1131294
Actin beta	Sigma	Cat# A3853; RRID:AB_262137
Insulin	Sigma	Cat# I2018; RRID:AB_260137
Glucagon	Agilent	Cat# A0565; RRID:AB_10013726
Adenoviruses		
Ad-GFP-U6-m-KIF3A-shRNA	Vector Biolabs	20170912T#2
Ad-GFP-U6-scmb-shRNA	Vector Biolabs	20160614T#5
Ad-GFP-m-KIF3A	Vector Biolabs	20180724T#7
Ad-CMV-NULL	Vector Biolabs	20150623t#7
Ad-GFP-U6-h-KIF3A-shRNA	Vector Biolabs	20180710T#20

CONTACT FOR REAGENT AND RESOURCE SHARING

Further information and requests for resources and reagents should be directed to and will be fulfilled by the Lead Contact, Anette Schürmann (schuermann@dife.de).

EXPERIMENTAL MODEL AND SUBJECT DETAILS

Animals

Male NZO/HIBomDife and B6.V-*Lep^{ob/ob}*/JBomTac (B6-ob/ob) mice (Charles River) were used and housed as described (Kluth et al., 2015). Similarly, the experimental setup was performed according to the protocol of Kluth et al. (2015). Briefly, starting at the age of 5 weeks onward, all mice received a carbohydrate-free diet (-CH, Altromin C105789). At the age of 18 \pm 1 weeks, one subgroup of animals was sacrificed for either pancreas removal or islet isolation. Another subgroup received a carbohydrate-containing diet (+CH, self-made with 40% carbohydrates) for 48 hours and were then sacrificed for pancreas removal or islet isolation (Kluth et al., 2015).

All animals were kept in accordance with the NIH guidelines for the care and use of laboratory animals. All experiments were approved by the animal welfare committees of the DIFE and the Ethics Committee of the State Ministry of Agriculture, Nutrition and Forestry (State of Brandenburg, Germany). The approval number is: V3- 2347-26-2014. The pancreatic islet donor or her/his relatives had given their consent to donate organs for medical research upon admission to intensive care unit. All procedures were approved by ethics committees at Uppsala and Lund Universities, Sweden (Approval number: 2011263).

Cell lines

The MIN6 cell line was kindly provided by Professor Jun-ichi Miyazaki from Japan.

Adenoviruses

Adenoviruses for the manipulation of KIF3A expression were purchased at Vector Biolabs (Malvern, USA).

Human islets

Human pancreatic islets of 213 donors (178 nondiabetics, 35 diagnosed with T2D) were included in this study and provided by the Nordic Network for Islet Transplantation, Uppsala University, Sweden (<http://www.nordicislets.org>).

METHOD DETAILS

Isolation of pancreatic islets and transcriptome analysis

Isolation of islets was performed as described (Kluth et al., 2015). At least 100 islets per animal of 3 B6-ob/ob versus 3 NZO mice were collected for total RNA preparation and transcriptome analysis. Islet RNA preparation was performed with the RNAqueous-Micro Kit (Thermo Fisher Scientific, AM1931, Waltham, USA) and quality was assessed with a Bioanalyzer (minimal RNA integrity: 8.0). Islet transcriptomes were determined via a Whole Mouse Genome DNA-Microarray (Agilent Technologies 4x44K chip, ImaGenes, Berlin, Germany).

Glucose-stimulated insulin secretion in primary mouse islets

65 freshly isolated pancreatic islets per mouse were used for perfusion experiments. Islets were equilibrated in Krebs-Ringer buffer (KRBH; 115 mmol/l NaCl, 4.5 mmol/l KCl, 2.6 mmol/l CaCl₂, 1.2 mmol/l KH₂PO₄, 1.2 mmol/l MgSO₄, 0.8 mmol/l NaHCO₃, 0.2% BSA, pH 7.4) under low glucose conditions (2.8 mmol/l) for 30 min and transferred into perfusion chambers with a continuous flow of 0.5 ml/min. Glucose-stimulated insulin secretion was measured continuously under low glucose conditions, high glucose conditions (20 mmol/l), then again with low glucose and finally with 40 mmol/l KCl for 18, 35, 30, and 20 min, respectively. Fractions were collected in 2 to 6 min intervals. Insulin levels were measured using the Ultrasensitive Insulin ELISA (Alpco Diagnostics, Salem, USA) and normalized to DNA content (Quant-iT PicoGreen dsDNA Assay Kit, Invitrogen, Carlsbad, USA).

Histological and immunofluorescence staining of pancreatic sections and morphometry

Apoptotic cells in pancreatic islets of B6-ob/ob and NZO mice were detected using the ApopTag Plus Peroxidase *In Situ* Apoptosis Kit (Merck Millipore, Billerica, USA). Pancreases of B6-ob/ob and NZO mice which were either fed the -CH- or the +CH-diet for 2 days were prepared for immunohistochemistry as described (Kluth et al., 2015). Sections were incubated with primary antibodies against acetylated α -tubulin (1:500, T6793, Sigma, St. Louis, USA), E-Cadherin (1:200, 610181, BD Biosciences, San Jose, USA) and Ki-67 (1:1000, ab15580, Abcam) over night at 4°C. Primary antibodies were detected with fluorophore-labeled secondary antibodies at a dilution of 1:400 (Alexa Fluor 546, Alexa Fluor 488 and Alexa Fluor 633; Invitrogen) plus DAPI (1 μ g/ml) for 1 h at room temperature and documented with a confocal microscope (TCS SP8 X, Leica Microsystems). The numbers of cilia per islet were analyzed with the ImageJ software package (v1.51j8, NIH) via an unbiased stereological approach. Structures larger than 8 μ m in length were excluded from the analysis due to eventual false-positive signals from nerve fibers within islets (Rodriguez-Diaz et al., 2011). Mean \pm SEM values were calculated from randomly selected islets of 3–5 pancreases per mouse strain and feeding condition. Differences were calculated with an unpaired Student's t test and considered significant at $p < 0.05$.

Whole mount staining of murine islets and morphometry

Isolated islets of B6-ob/ob mice ($n = 30$) and NZO ($n = 28$) out of 3 animals per strain were fixed in 4% paraformaldehyde, washed in PBS and stained against Arl13b (1:100, 17711-1-AP, Proteintech, Rosemont, USA) and DAPI. Islets were mounted and imaged using a Leica SP5 confocal microscope. Z stacks of islets were analyzed with the Imaris8 software package (Bitplane, Zurich, Switzerland). Briefly, islets were defined based on DAPI-positive structures with an additional perimeter of 7 μ m to include whole cells.

Cell culture, transfection and BrdU assay in MIN6 and primary mouse and human islet cells

Mycoplasma-free mouse insulinoma 6 (MIN6) cells were cultured in Dulbecco's modified Eagle's medium (P04-03590, PAN-Biotech, Aidenbach, Germany) containing 10% heat-inactivated fetal calf serum (Life Technologies, Darmstadt, Germany) and 1% Penicillin/Streptomycin in a humidified incubator at 37°C and 5% CO₂.

Isolated B6 islets were recovered for 24 h, digested with HQTase Cell Detachment Solution (SV30030.01, GE Healthcare Life Sciences, Logan, USA). For shRNA-mediated suppression of KIF3A, MIN6 and primary islet cells were seeded in poly-L-lysine-coated 24-well cell culture plates on glass coverslips and transfected with adenoviruses expressing a *Kif3a*-specific shRNA (20170912T#2, Vector Biolabs) at a multiplicity of infection (MOI) of 250. As a control, cells were transfected with a scrambled shRNA-encoding adenovirus (20160614T#5, Vector Biolabs).

For KIF3A overexpression, MIN6 cells were transfected with a *Kif3a*-encoding adenovirus (20180724T#7, Vector Biolabs, MOI 250). Control cells were transfected with the appropriate control adenovirus (20150623T#7, Vector Biolabs).

For the rescue experiment, KIF3A expression was silenced using the *Kif3a*-shRNA-specific adenovirus and subsequently rescued with a plasmid encoding an optimized KIF3A sequence (GenScript, Piscataway, USA, see also Figure 6F). Five days after the transfection, MIN6 cells were incubated with BrdU (100 μ mol/l) for 2 h, primary islets cells (2 days after transfection) were incubated with BrdU for 24 h and fixed with 4% paraformaldehyde.

Human islets from 2 different male donors (Prodo Labs # HP-18320-01 and HP-19010-01) were purchased from tebu-bio (Le Perray en Yvelines, France) and cultured in PIM(S) media supplemented with PIM(G), PIM(ABS) and 1% Penicillin/Streptomycin

(Prodo Labs, Aliso Viejo, USA), dispersed and transfected with control (20160614T#5, Vector Biolabs) or *KIF3A*-encoding adenoviruses (20180710T#20, Vector Biolabs) at a MOI of 500. Dispersed human islet cells were treated with harmine (10 μ Mol/l in DMSO, 286044-1G, Sigma) and BrdU every other day for 4 days.

Immunocytochemistry was performed as described (Kluth et al., 2015). BrdU incorporation was detected using a primary antibody against BrdU (1:500, B8434, Sigma) and a fluorophore-labeled secondary anti-rat antibody (1:400, Alexa Fluor 546, Invitrogen). For MIN6, mouse and human islet experiments, in total more than 14,000, 6,000, and 1,200 cells per condition were counted, respectively.

Western Blot analysis

Western blot analysis was performed as described (Kluth et al., 2011) using a 12% polyacrylamide gel loaded with 10 μ g protein. Primary antibodies against KIF3A (1:1000; ab11259, Abcam, Cambridge, UK), acetylated α -tubulin (1:1000; T6793, Sigma), ADH1 (1:1000, 5295, Cell Signaling, Cambridge, UK), HMMR (1:1000, MBS 126929, MyBioSource, Vancouver, Canada), GAPDH (1:25000, AM4300, Thermo Fisher Scientific), Vinculin (1:1000, sc-73614, Santa Cruz, Dallas, USA) and actin (1:25000, A3853, Sigma) and appropriate horseradish peroxidase-conjugated secondary antibodies (1:20000, Dianova, Hamburg, Germany) were applied.

Human islet RNA sequencing

Gene expression in human islets was quantified by RNA sequencing. Isolation of total RNA was done using the AllPrep DNA/RNA kit (QIAGEN) and quality of isolated RNA was assessed by 2100 Bioanalyzer (Agilent Technologies) or 2200 TapeStation (Agilent Technologies). The quantity was measured on a NanoDrop 1000 (NanoDrop Technologies) or a Qubit 2.0 Fluorometer (Life Technologies). 1 μ g of total RNA of sufficient quality (RIN > 8) and a TruSeq RNA sample preparation kit (Illumina) were used for sample preparation. Size selection was done using Agencourt AMPure XP beads (Beckman Coulter) aiming at a fragment size above 300 bp. Libraries were quality controlled on a 2200 TapeStation (Agilent Technologies) before they were sequenced on a HiSeq 2000 (Illumina). The raw RNaseq data were base called and de-multiplexed using CASAVA 1.8.2 (Illumina) before alignment to hg19 with STAR. To count the number of reads aligned to specific transcripts featureCounts (<http://bioinf.wehi.edu.au/featureCounts/>) was used. Raw data was normalized using trimmed mean of M-values and transformed using voom (limma R-package). Expression data were expressed as log2counts per million (log2 CPM). Linear regression analyses were performed with all 297 human orthologs (covariates: age and gender) to calculate beta-coefficients and nominal p values. A positive value means upregulation in T2D and vice versa.

QUANTIFICATION AND STATISTICAL ANALYSIS

Statistical significance was analyzed using the Student's t test, one-way ANOVA or two-way ANOVA by comparing the test groups with the appropriate control groups. Data are presented as mean values \pm SEM. P values are indicated with single asterisk (* < 0.05), double asterisks (** < 0.01) and triple asterisks (***) < 0.001. The n number for each experiment has been stated in figure legends.

Normalized DNA-microarray based transcriptome data were obtained for 32837 transcripts (Images). Differentially expressed genes (DEGs) were specified with an ENSEMBL gene-ID, a log2 fold change (log2FC) > |1.5| (> 2.8-fold up- or downregulation) and p < 0.05. Differentially expressed cilia genes were identified by overlapping with 5266 orthologs of cilia-annotated genes for the species *M. musculus*, *H. sapiens* and *R. norvegicus* in the database Cildb (<http://cildb.cgm.cnrs-gif.fr/>) (Arnaiz et al., 2009, 2014). A significant enrichment of cilia genes among DEGs in islets of NZO and B6-ob/ob mice was calculated by permutation analysis with the 32,837 transcripts (100,000 permutations). A Pearson's Chi-square test (χ^2) was used to calculate the expected distribution and a p value.

For the identification of biological processes to be affected by differentially expressed cilia genes we used the web-based GOrilla application (2017/10/07) (<http://cbl-gorilla.cs.technion.ac.il>) to identify enriched GO terms (enrichment p value < 10^{-3}) from ranked gene lists (log2FC) of the 327 differentially expressed cilia genes (2-day +CH-feeding) in NZO and B6-ob/ob islets. Enrichment p values were calculated with a minimum-hypergeometric test (Eden et al., 2009). A circular visualization of enriched GO terms in B6-ob/ob was generated with the software R (v.3.4.2) (R Core Team, 2017) and a GOcircle-script (GOplot 1.0.2) (<http://wencke.github.io/>). Z-scores were calculated by the quotient of upregulated minus downregulated genes and the square root of all considered genes (Walter et al., 2015). Ranked visualization of altered GO terms was generated with p value thresholds of < 10^{-7} for B6-ob/ob and < 10^{-4} for NZO.

For the determination of compliances between differentially expressed cilia genes in mice and humans, transcriptome data from islets of diabetic and non-diabetic human donors were compared. A study population of 213 non-diabetic and diabetic human islet donors from the Nordic network for clinical islet transplantation was used to overlap expression data (Ottosson-Laakso et al., 2017) of 297 human orthologs with differentially expressed cilia genes between NZO and B6-ob/ob mice (2 day +CH-feeding).

DATA AND SOFTWARE AVAILABILITY

All data used in this manuscript are available upon request. The accession number for the raw mouse islet microarray data is GEO: GSE64956. Accession numbers for raw human RNaseq data are Databases: GEO: GSE50244, GSE108072.

Supplemental Information

**Decreased Expression of Cilia Genes in
Pancreatic Islets as a Risk Factor for Type 2
Diabetes in Mice and Humans**

Oliver Kluth, Mandy Stadion, Pascal Gottmann, Heja Aga, Markus Jähnert, Stephan Scherneck, Heike Vogel, Ulrika Krus, Anett Seelig, Charlotte Ling, Jantje Gerdes, and Annette Schürmann

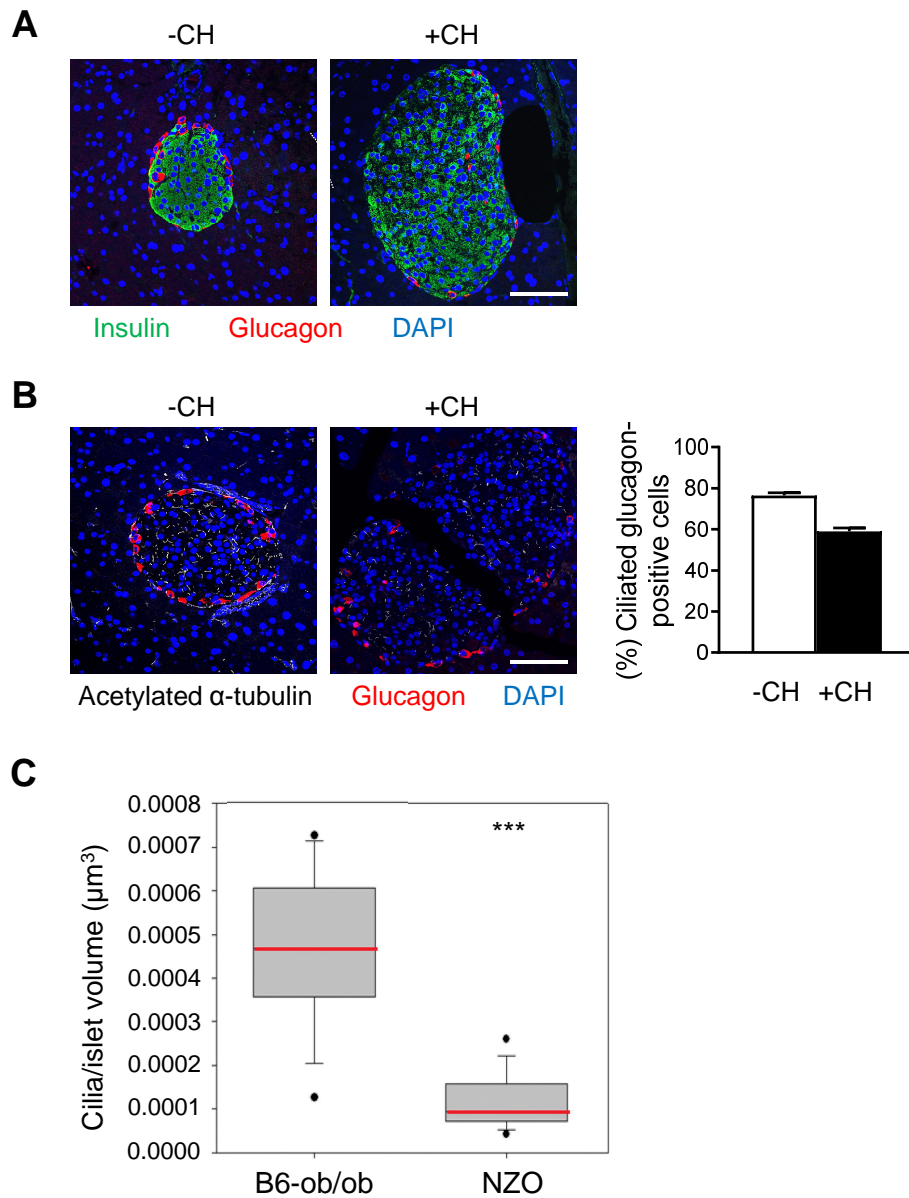


Figure S1. Ciliation of whole mounted islets of B6-ob/ob and NZO mice. Related to Figure 3.

(A) Representative insulin and glucagon co-staining in pancreatic islets of B6-ob/ob mice fed without carbohydrates (-CH) or 2 days after the carbohydrate intervention (+CH), $n = 2$ mice per condition. Scale bar, 50 μM .

(B) Representative acetylated α -tubulin and glucagon co-staining in pancreatic islets of B6-ob/ob mice fed without carbohydrates (-CH) or 2 days after the carbohydrate intervention (+CH) with corresponding quantification, $n = 2$ mice per condition. Scale bar, 50 μM .

(C) Quantification of beta-cell primary cilia of whole mounted B6-ob/ob and NZO islets stained for the cilia marker Arl13b (maximum projection). Data are mean \pm SD, *** $p < 0.001$.

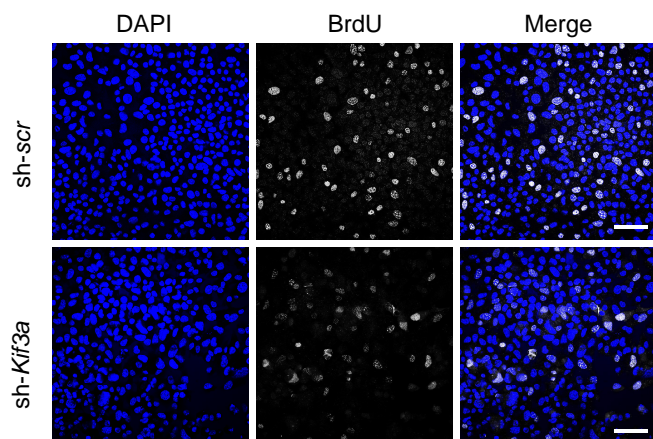


Figure S2. Adenoviral-mediated suppression of *Kif3a* in MIN6 cells reduces the incorporation of BrdU. Related to Figure 6.

Representative immunocytochemical stains of MIN6 cells transfected with scrambled control (sh-scr) or *Kif3a*-specific (sh-*Kif3a*) adenovirus stained for DAPI (left panel) and BrdU (middle panel) with the respective merge (right panel). Multiplicity of infection (MOI): 250, scale bars, 20 μ m.

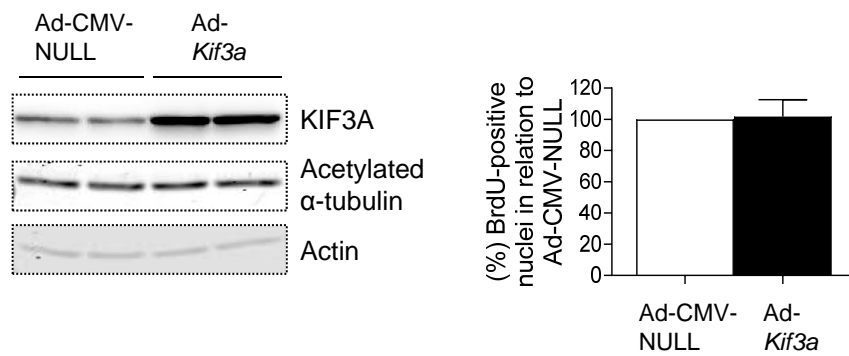


Figure S3. Adenoviral-mediated overexpression of *Kif3a* does not alter beta-cell proliferation. Related to Figure 6.

KIF3A was overexpressed in the MIN6 beta-cell line (left panel, MOI 250) and proliferation capacity was assessed via BrdU incorporation (right panel). Actin was used as loading control.

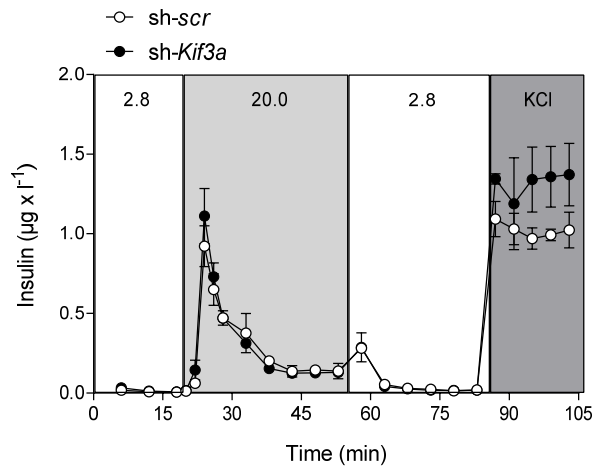


Figure S4. Adenoviral-mediated suppression of *Kif3a* does not affect glucose-stimulated insulin secretion in primary mouse islets. Related to Figure 6.

Primary mouse islets of B6 animals were infected with scrambled control (sh-scr) or *Kif3a*-specific (sh-*Kif3a*) adenovirus and 24 h later perfusion experiments were performed (MOI 5,000, 100 islets per group, n = 2).

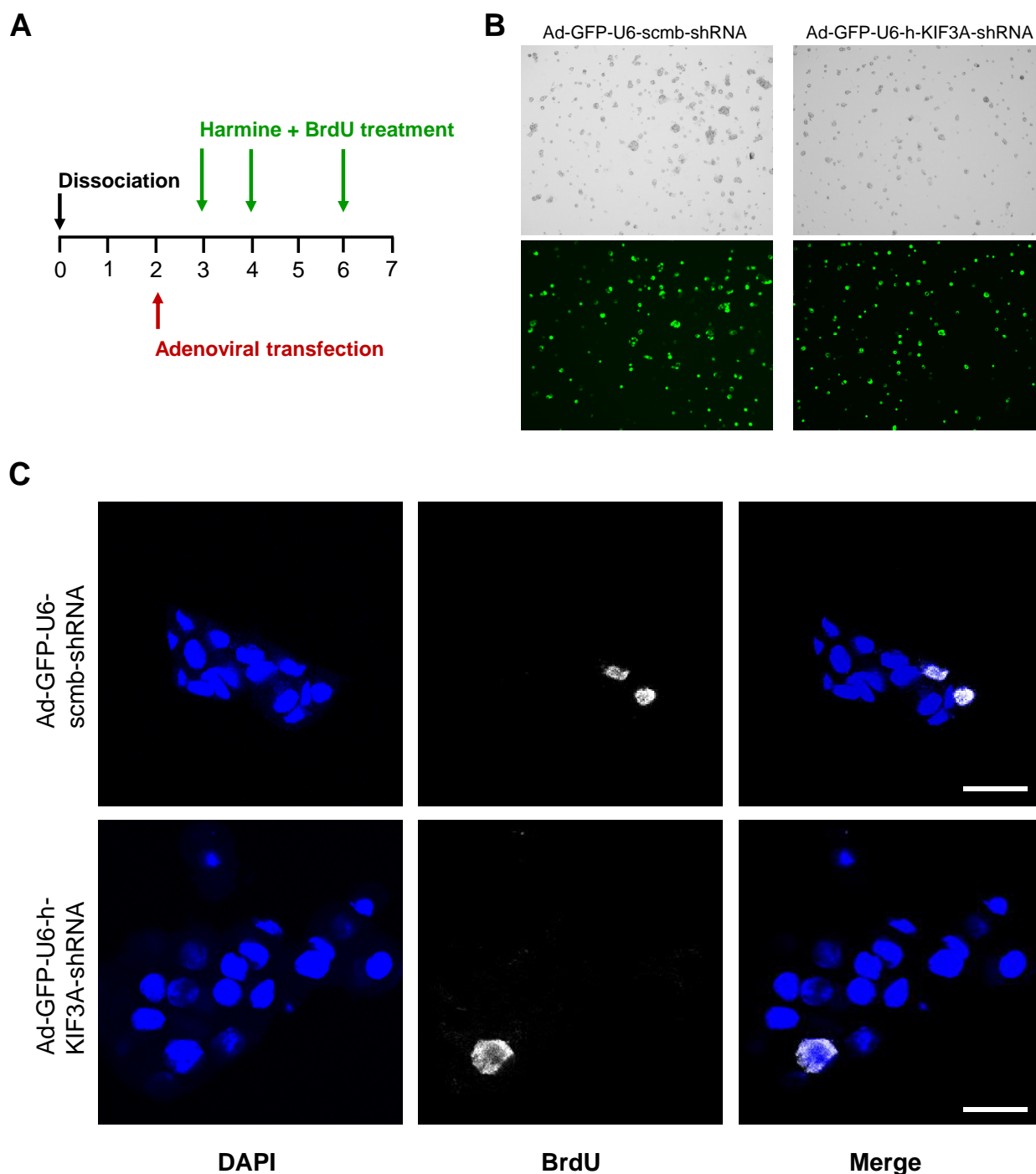


Figure S5. Silencing of KIF3A in primary human islet cells. Related to Figure 6.

(A) Primary human islet cells were dispersed and transfected with control or *KIF3A*-specific adenovirus (multiplicity of infection: 500) and treated with harmine and BrdU for 4 days.

(B) 24 h after infection, transfection efficiency in control (Ad-GFP-U6-scmb-shRNA) and *KIF3A*-depleted (Ad-GFP-U6-h-KIF3A-shRNA) islet cells was recorded via the detection of GFP fluorescence.

(C) Representative images of BrdU-positive nuclei in dispersed primary human islet cells 5 days after *KIF3A* suppression. Scale bar, 20 μ m.